Internuclear-distance dependence of the role of excited states in high-order-harmonic generation of H_2^+

Yong-Chang Han
Department of Physics and Astronomy, Aarhus University, DK-8000 Aarhus C, Denmark and
School of Physics and Optoelectronic Technology, Dalian University of Technology, Dalian 116024, China

Lars Bojer Madsen
Department of Physics and Astronomy, Aarhus University, DK-8000 Aarhus C, Denmark
(Received 24 January 2013; published 5 April 2013)

The interference minimum in the high-order harmonic spectrum of H_2^+ is studied by solving the full three-dimensional time-dependent Schrödinger equation for the electronic motion keeping the nuclei fixed. The two-center interference model works well when the internuclear distance is around its equilibrium value where also recombination to the $^2\Sigma_g^+$ $(1s\sigma_g)$ ground state dominates. As the internuclear distance is increased, the minimum first shifts in position compared with the prediction of the two-center interference model and subsequently disappears. These effects are caused by the excited $^2\Sigma_u^+$ $(2p\sigma_u)$ state, partly due to the interference between the amplitudes of recombination to the ground and excited states, but also partly due to the signal associated with recombination to the excited state alone. We find that at internuclear distances beyond $R \simeq 3$ a.u. the signal close to the harmonic cutoff may be completely dominated by recombination into the excited $^2\Sigma_u^+$ $(2p\sigma_u)$ state.

DOI: 10.1103/PhysRevA.87.043404 PACS number(s): 32.80.Wr, 42.65.Ky, 42.50.Hz

I. INTRODUCTION

When matter interacts with an intense femtosecond laser pulse, emission of coherent uv or xuv radiation may follow through the process of high-order-harmonic generation (HHG) [1,2]. The semiclassical three-step model is typically used to explain the main physics in this process [3–5]. First, an electron escapes into the continuum due to the presence of the external field. Then, the electron is accelerated in the electric field, initially away and then back towards the parent ion. Finally, the electron may recombine with the parent ion with emission of high-frequency coherent radiation. Apart from the interest in HHG as a source for coherent radiation extending into the xuv regime, HHG can be used to generate attosecond pulses [6–10] and to obtain information about molecular structure and orbitals (see, e.g., Refs. [11–23].)

A characteristic of harmonic spectra is the presence of a minimum. The numerical investigation of H_2^+ has shown that the minimum position of the HHG spectrum depends on the molecular alignment, β, with respect to the laser polarization direction [13]. The minimum is ascribed to an interference between the radiation emitted from the two nuclear centers based on a description of the ground state in terms of a linear combination of atomic orbitals and of the electronic continuum in terms of plane waves [14,16]. The interference structure in this two-center interference model is related to the internuclear distance R, the angle β, and the symmetry of the highest occupied molecular orbital (HOMO). For a HOMO of gerade symmetry, the two-center interference is governed by

$$I(\boldsymbol{k}) = e^{-i\boldsymbol{k}\cdot\boldsymbol{R}/2} + e^{i\boldsymbol{k}\cdot\boldsymbol{R}/2} = 2\cos(\boldsymbol{k}\cdot\boldsymbol{R}/2), \qquad (1)$$

where $\boldsymbol{R}$ describes the position of the nuclei and $\boldsymbol{k}$ is the wave vector of the returning electron before recombination. Two-center interference minima are expected to occur when the argument of the cosine in Eq. (1) is an odd multiple of $\pi/2$, i.e., following the formula (here and throughout atomic units are used)

$$\begin{aligned} kR\cos\beta &= (2n+1)\pi, \quad n = 0,1,2,\ldots, \\ N_{\text{min-TI}}\omega_0 &= k^2/2, \end{aligned} \qquad (2)$$

where k is the electron momentum, $N_{\text{min-TI}}$ is the harmonic order of the two-center interference minimum, and ω_0 is the center angular frequency of the laser field. The two-center interference model was, for example, used to explain the minima in the HHG spectrum of H_2^+ calculated by the time-dependent Schrödinger equation (TDSE) [14,16] and the model was extended to take nuclear motion into account [15,17]. In the conventional two-center interference model, it is assumed that the electron escapes from the HOMO and later recombines to the HOMO. In addition to the effects relating to the HOMO, it was found for multielectron molecules that the states lying energetically below the HOMO can contribute to the HHG spectrum [18–22]. We previously demonstrated that the electronic bound states lying energetically *above* the HOMO can also influence the HHG spectrum, and the interference between the amplitudes describing recombination into the electronic ground and excited states, respectively, may give rise to a minimum in the HHG spectrum [24]. Effects of excited states in the cation in many-electron molecules have also been investigated and shown to modify the spectra [25,26]. The relation between two-center interference minima and ellipticity of the generated light was investigated in Ref. [27]. The role of the lowest unoccupied orbital was investigated in Ref. [28] in a modified version of the strong-field approximation.

In this work, we investigate the effect of the excited states in H_2^+ with varying internuclear distance on the HHG spectrum. Taking H_2^+ as an example, we perform full three-dimensional (3D) (for $\beta \neq 0$) TDSE calculations for the electronic part. We vary the internuclear distance from equilibrium to somewhat larger distances, while adjusting β according to the two-center interference formula of Eq. (2) to keep fixed the same position

of the predicted interference minimum. We find that the two-center interference model works well in the vicinity of the equilibrium, where there is no strong coupling between the $^2\Sigma_g^+$ ($1s\sigma_g$) ground state (σ_g in short) and the $^2\Sigma_g^+$ ($2p\sigma_u$) first excited state (σ_u in short), while with increasing internuclear distance the coupling becomes more important, and recombination into the σ_u state and the interference between the amplitudes for recombination to the σ_g and the σ_u states need to be accounted for. In a recent one-dimensional study of H_2, a similar decomposition for the H_2^+ states was used [29].

The paper is organized as follows. In Sec. II, we describe the theoretical model used to explain the effect of excited states on the harmonic spectrum. In Sec. III, we discuss the results, and in Sec. IV we present our conclusions.

II. THEORY

The HHG spectrum is modeled by the signal from a single molecule. This signal is related to the absolute square of the Fourier transform of the dipole acceleration and by invoking Ehrenfest's theorem; an expression for the spectrum reads [30,31]

$$S_{\rm tot}(\omega) = \left| \int \hat{\boldsymbol{e}} \cdot \langle \ddot{\boldsymbol{d}}(t) \rangle e^{i\omega t} dt \right|^2 = \left| \int \hat{\boldsymbol{e}} \cdot \{ \langle \psi_{\rm tot}(\boldsymbol{r},t) | \nabla V(\boldsymbol{r}) | \psi_{\rm tot}(\boldsymbol{r},t) \rangle + \boldsymbol{F}(t) \} e^{i\omega t} dt \right|^2, \tag{3}$$

where $\hat{\boldsymbol{e}}$ denotes the polarization direction, $V(\boldsymbol{r})$ is the molecular potential at the electronic coordinate $\boldsymbol{r}$, and $\boldsymbol{F}(t)$ is the electric field. The last line in Eq. (3) shows that the spectrum is mainly dependent on the first term of the right-hand side, i.e., the time-dependent expectation value of the gradient of the potential, $\langle \psi_{\rm tot}(\boldsymbol{r},t) | \nabla V(\boldsymbol{r}) | \psi_{\rm tot}(\boldsymbol{r},t) \rangle$.

We consider the TDSE in the length gauge to obtain the wave packet, $\psi_{\rm tot}(\boldsymbol{r},t)$, at time t (see Ref. [32] for a discussion of the calculation of HHG in the velocity gauge):

$$i \frac{\partial}{\partial t} \psi_{\rm tot}(\boldsymbol{r},t) = \left(-\frac{\nabla^2}{2} + V(\boldsymbol{r}) + \boldsymbol{r} \cdot \boldsymbol{F}(t) \right) \psi_{\rm tot}(\boldsymbol{r},t). \tag{4}$$

We substitute $\psi_{\rm tot}(\boldsymbol{r},t) = \frac{1}{r} \varphi_{\rm tot}(\boldsymbol{r},t)$ into Eq. (4) and obtain for the reduced wave function

$$i \frac{\partial}{\partial t} \varphi_{\rm tot}(\boldsymbol{r},t) = \left(-\frac{1}{2} \frac{\partial^2}{\partial r^2} + \frac{L^2}{2r^2} + V(\boldsymbol{r}) + \boldsymbol{r} \cdot \boldsymbol{F}(t) \right) \varphi_{\rm tot}(\boldsymbol{r},t), \tag{5}$$

with L^2 being the square of the angular momentum operator. We expand $\varphi_{\rm tot}(\boldsymbol{r},t)$ in spherical harmonics $Y_{lm}(\theta,\phi)$ with radial functions $f_{lm}(r,t)$, which are found using grid methods [33,34].

$$\varphi_{\rm tot}(r,\theta,\phi,t) = \sum_{l=0}^{L_{\rm max}} \sum_{m=-l}^{l} f_{lm}(r,t) Y_{lm}(\theta,\phi). \tag{6}$$

In H_2^+ the nuclei are fixed at $\pm \boldsymbol{R}/2$ and the molecule interacts with a linearly polarized external field.

Our analysis of the role of the excited σ_u state is facilitated by splitting $\psi_{\rm tot}(\boldsymbol{r},t)$ into the following components:

$$\psi_{\rm tot}(\boldsymbol{r},t) = c_g(t)\psi_g(\boldsymbol{r}) + c_u(t)\psi_u(\boldsymbol{r}) + \psi_{\rm res}(\boldsymbol{r},t), \tag{7}$$

where $\psi_g(\boldsymbol{r})$ and $\psi_u(\boldsymbol{r})$ denote the orbitals of the σ_g ground state and the σ_u first excited state, respectively. The wave packet $\psi_{\rm res}(\boldsymbol{r},t)$ represents the residual part of $\psi_{\rm tot}(\boldsymbol{r},t)$, including other excited states and the electronic two-center continuum. In Eq. (7) the complex amplitude $c_{g(u)}(t)$ contains both the energy phase factor, $e^{-iE_{g(u)}t}$, and the time-dependent amplitude due to interaction with the external field. We substitute Eq. (7) into Eq. (3) and maintain what we have checked are the dominating terms and obtain

$$S_{\rm tot}(\omega) \simeq S_g(\omega) + S_u(\omega) + 2[A_g^*(\omega)A_u(\omega)], \tag{8}$$

with $S_g(\omega) = |A_g(\omega)|^2$, $S_u(\omega) = |A_u(\omega)|^2$, and

$$A_g(\omega) = \hat{\boldsymbol{e}} \cdot \int 2{\rm Re}\langle c_g(t)\psi_g(t)|\nabla V(\boldsymbol{r})|\psi_{\rm res}(t)\rangle e^{i\omega t} dt,$$
$$A_u(\omega) = \hat{\boldsymbol{e}} \cdot \int 2{\rm Re}\langle c_u(t)\psi_u(t)|\nabla V(\boldsymbol{r})|\psi_{\rm res}(t)\rangle e^{i\omega t} dt. \tag{9}$$

Equation (8) shows that the HHG spectrum includes recombination to the σ_g state, $S_g(\omega)$, recombination to the σ_u state, $S_u(\omega)$, and the interference term between these two components, $2{\rm Re}[A_g^*(\omega)A_u(\omega)]$. We refer to the interference term as the *orbital interference term*. In the two-center interference model the contribution $S_u(\omega)$ and the orbital interference term are absent. In the following, we analyze the HHG spectra in terms of the components of Eq. (8) for different internuclear distances to investigate the role of the excited σ_u state, and we compare the result for the minimum by the full TDSE calculation [Eq. (3)] with the prediction by the two-center interference model.

III. RESULTS AND DISCUSSIONS

Calculations have been performed for a pulse with an 800 nm wavelength (angular frequency, $\omega_0 = 0.057$), a trapezoidal shape, and a total duration of 7 optical cycles and linear ramps of 1.5 optical cycles. The laser peak intensity was 1.7×10^{14} W/cm^2. We varied the internuclear distance R and the alignment angle β together according to Eq. (2) to fix the two-center interference minimum at $N_{\text{min-TI}} = 29$. We consider the spectrum along the laser polarization direction (see Refs. [27,35,36] and references therein for a discussion of polarization properties of HHG radiation). In the calculation, we used an equidistant grid with 1536 points that extended up to 125 a.u. and an angular basis set with $L_{\rm max} = 41$. The calculations were repeated in a larger box (2048 points in 160 a.u.) with a larger angular basis ($L_{\rm max} = 46$), and the results were converged.

In the left panels of Fig. 1, the HHG spectra calculated by Eq. (3) are shown for $R = 2.0$, 2.5, 3.0, and 3.25 a.u., with β correspondingly taken to be 30°, 46°, 55°, and 58°. We calculated the smoothed spectrum $\int S(\varpi)\exp(-(\varpi - \omega)^2/\sigma^2)d\varpi$, with $\sigma = 3\omega_0$ [14], as shown by the solid red curves to obtain a good estimate of the minimum position. The position of the interference minimum coincides with the anticipation of the two-center interference formula, i.e.,

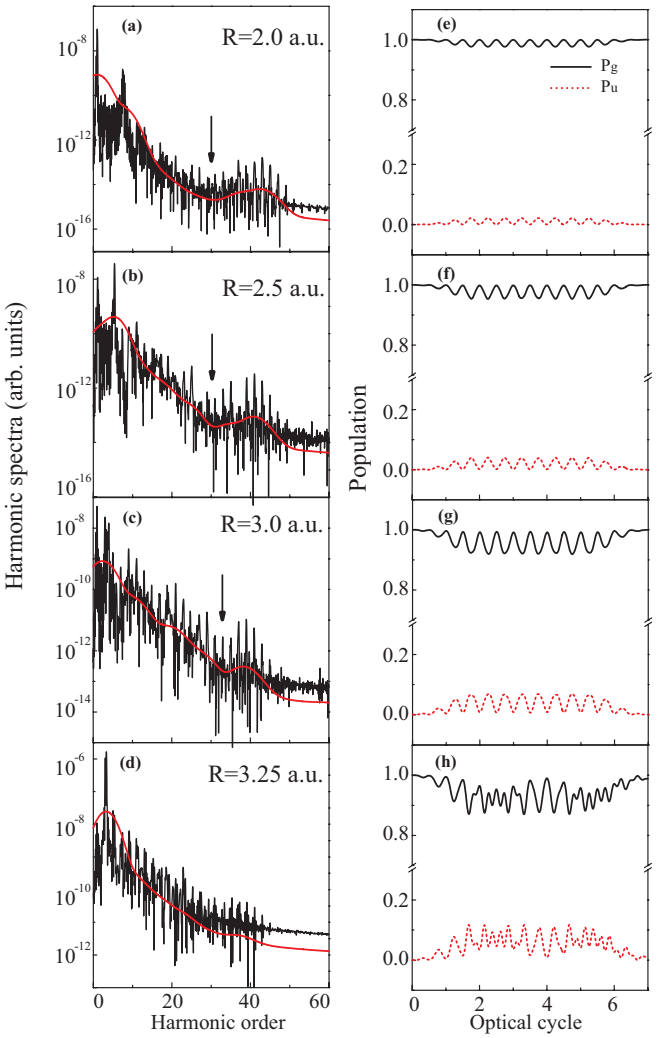

FIG. 1. (Color online) The HHG spectrum of H_2^+ (left panels) and the corresponding time-dependent populations in the σ_g and σ_u states (right panels). The internuclear distance R and the alignment angle β are as follows: (a) $R = 2.0$ a.u. and $\beta = 30^\circ$, (b) $R = 2.5$ a.u. and $\beta = 46^\circ$, (c) $R = 3.0$ a.u. and $\beta = 55^\circ$, and (d) $R = 3.25$ a.u. and $\beta = 58^\circ$. The arrow points to the location of the interference minimum. The peak intensity of the seven-cycle laser pulse is 1.7×10^{14} W/cm^2, and the wavelength is 800 nm.

$N_{\text{min-TI}} = 29$ in Figs. 1(a) and 1(b) for $R = 2.0$ and 2.5 a.u. Figure 1(c) shows that for $R = 3.0$ a.u. the minimum occurs at harmonic order 33 which is larger than expected by Eq. (2). Figure 1(d) shows that at $R = 3.25$ a.u. the minimum can hardly be observed. So the two-center interference model gradually fails to explain the actual form of the harmonic spectrum with increasing internuclear distance.

We turn back to a consideration of the physics included in the full TDSE calculation, but left out in the analysis leading to the two-center interference model, in order to understand these results. The coupling between the ground and the first excited states becomes increasingly important for increasing internuclear distance [37], and hence the first excited state plays a more and more decisive role, and in addition, the residual wave packet $\psi_{\text{res}}(\boldsymbol{r},t)$ in Eq. (7) contains more high-excited states as well as the multicenter Coulombic continuum, which cannot be simply treated as a plane wave assumed in the derivation of the two-center interference formula (2). As a result, the increase of the internuclear distance finally leads to the failure of the two-center interference model. The following analysis based on an inspection of the populations and the behavior of the components in Eq. (8) confirms these conclusions.

The time-dependent populations in the σ_g and the σ_u states, $P_{g(u)}(t) = |\langle\psi_{g(u)}(\boldsymbol{r})|\psi_{\text{tot}}(\boldsymbol{r},t)\rangle|^2$, are shown in the right-hand panels of Fig. 1 for the cases corresponding to the spectra in the left column. Nonresonant variations in the populations are seen during the pulse, and the amplitude of these changes increases with the internuclear distance. This behavior results from the increase of the transition dipole moment between the σ_g and σ_u states [37]. Figure 1 shows that the population at the beginning and the end of the pulse mainly resides in the σ_g state. During the pulse, however, when recombination occurs and harmonics are emitted, the σ_u state plays a role, and it becomes increasingly important with increasing internuclear distance. The temporary population of σ_u is small compared to the population of the σ_g state, but we now show that the effect of the recombination into the σ_u state is important, especially for the plateau region of the HHG spectrum, where it may dominate the spectrum.

In order to elucidate the detailed information contained in the HHG spectrum, we perform a component analysis according to Eqs. (8) and (9) for the spectra of Fig. 1. Figure 2 shows the corresponding smoothed spectra components. The notation $S_{\text{tot}}(\omega)$ [see legend in Fig. 2(a)] is used to represent the total HHG spectrum, which is dominated by three components: $S_g(\omega)$, representing the contribution of the recombination to the σ_g state; $S_u(\omega)$, representing the contribution of the recombination to the σ_u state; and the third component is the orbital interference term, $2\text{Re}[A_g^*(\omega)A_u(\omega)]$ in Eqs. (8) and (9). So, by comparing $S_{\text{tot}}(\omega)$ with $S_g(\omega) + S_u(\omega)$, we demonstrate the effect of the third component, the orbital interference term.

Figures 2(a) and 2(b) show that $S_g(\omega)$ dominates the HHG spectrum in the vicinity of the equilibrium distance. Both $S_g(\omega)$ and $S_{\text{tot}}(\omega)$ present minima at $N_{\text{min-TI}} = 29$, in accordance with the expectation based on the two-center interference formula of Eq. (2), while the $S_u(\omega)$ component does not affect the shape. Accordingly, the effect of the orbital interference term is negligible, and the spectra of $S_{\text{tot}}(\omega)$ and $S_g(\omega) + S_u(\omega)$ are almost on top of each other.

The ionization probability increases and the recombination into the σ_u state becomes more important at $R = 3$ a.u. due to the increase of the temporary population of the σ_u state. Figure 2(c) shows that the contributions of $S_g(\omega)$ and $S_u(\omega)$ are comparable in the plateau region. For the harmonic order from 0 to 30, $S_g(\omega)$ is higher than $S_u(\omega)$, while for the harmonic order from 30 to 40, $S_u(\omega)$ is higher than $S_g(\omega)$. In addition, in $S_g(\omega)$, the two-center interference minimum cannot be observed. This is because $\psi_{\text{res}}(\boldsymbol{r},t)$ in Eq. (9) cannot be approximated by a simple plane wave in this case, but contains excited states and the two-center Coulombic continuum. The minimum shown in $S_{\text{tot}}(\omega)$ is located at harmonic order 33, and it comes from the orbital interference. We also see that the two spectra corresponding to $S_{\text{tot}}(\omega)$ and $S_g(\omega) + S_u(\omega)$ are no longer on top of each other, and a suppression of $S_{\text{tot}}(\omega)$ around harmonic

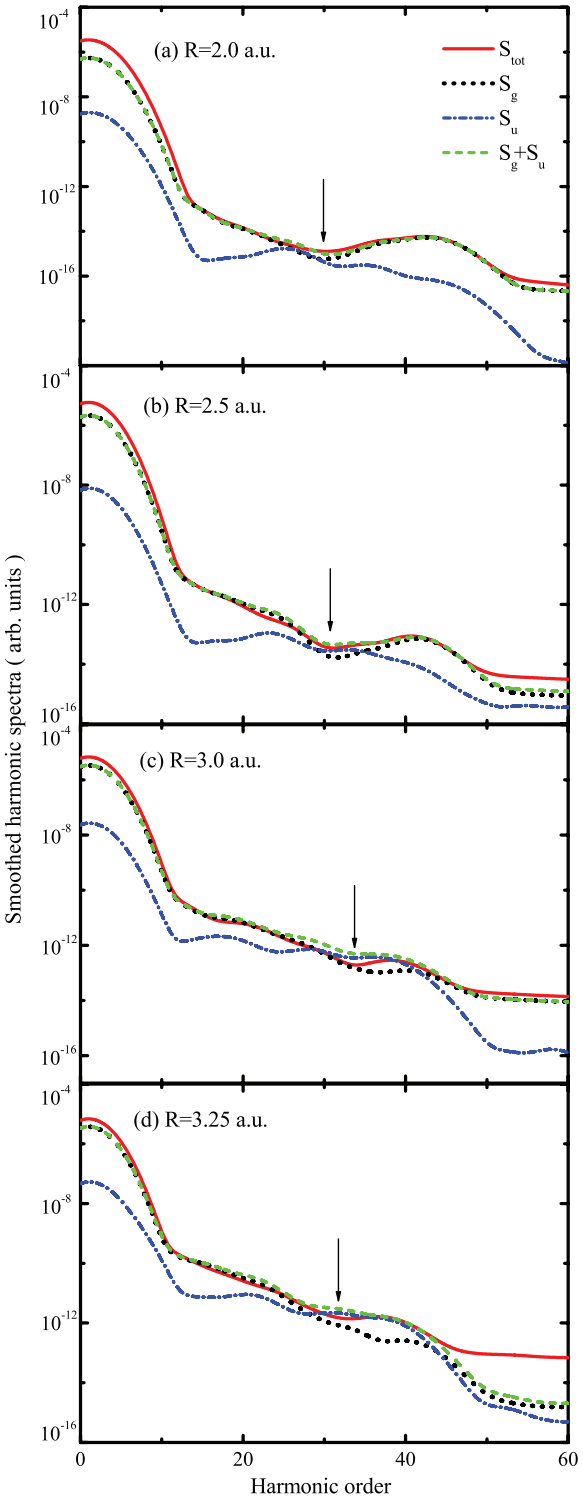

FIG. 2. (Color online) The smoothed spectra components of the HHG spectra of Fig. 1. The arrow points to the location of the orbital interference minimum.

order 33 can be clearly observed. We can therefore conclude that, at $R = 3.0$ a.u., the $S_u(\omega)$ and the orbital interference terms play important roles in the HHG spectrum and that the minimum of the spectrum comes from orbital interference.

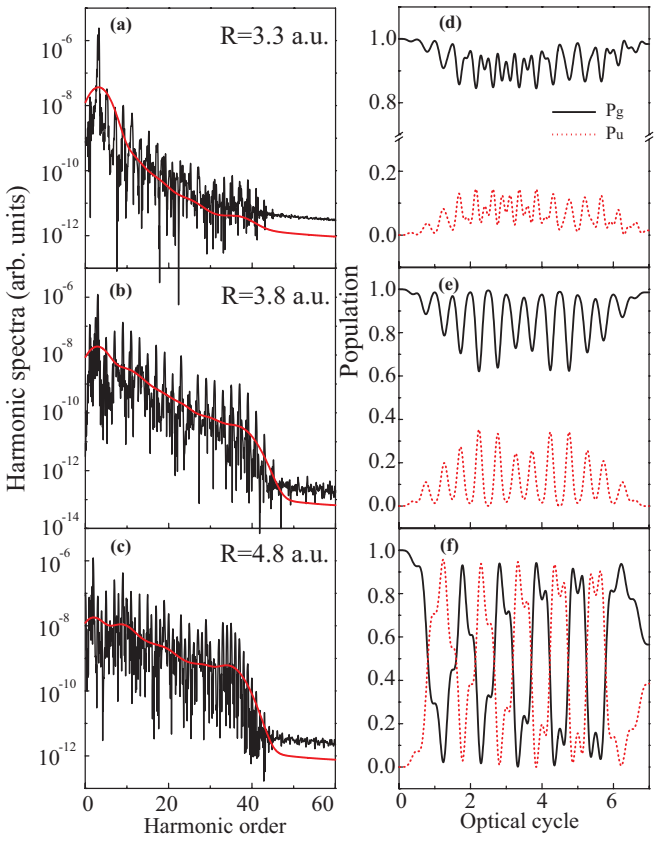

FIG. 3. (Color online) As Fig. 1, except the sets of R and β are as follows: (a) $R = 3.3$ a.u. and $\beta = 58.5°$, (b) $R = 3.8$ a.u. and $\beta = 63°$, and (c) $R = 4.8$ a.u. and $\beta = 69°$, corresponding to the distances of the three-photon, two-photon, and one-photon resonances, respectively, between the σ_g and σ_u states. In panels (d), (e), and (f) the populations in the ground state, P_g and first excited state, P_u are shown during the pulse.

The contributions to the spectrum from the different components are illustrated in Fig. 2(d) for $R = 3.25$ a.u. This distance is near the region of the three-photon resonance between the σ_g and the σ_u state, which results in a relatively stronger coupling between the two bound states. The two-center interference minimum can hardly be observed from $S_g(\omega)$. This is similar to the case in Fig. 2(c). Although the orbital interference in the $S_{tot}(\omega)$ is not obvious, by comparing $S_g(\omega) + S_u(\omega)$ to $S_{tot}(\omega)$, we can still locate a suppression of the HHG spectrum around the harmonic order of 31. The signal associated with recombination to the σ_u state completely dominates the spectrum between harmonics 35 and 40.

In Fig. 3, R is increased to 3.3, 3.8, and 4.8 a.u., which corresponds to the distances of three-photon, two-photon, and one-photon resonance conditions, respectively, between the σ_g and the σ_u states. The corresponding alignment angles for the three cases are 58.5°, 63.0°, and 69°. Figure 3 shows that the two-center interference minimum cannot be observed in the total HHG spectra for any of these cases. The time-dependent populations of the σ_g and σ_u states are shown in the right-hand panels of Fig. 3. With the increase of R, the coupling between the two bound states becomes much stronger, with the most pronounced Rabi oscillations in the one-photon resonance case, and in addition, the ionization potential decreases

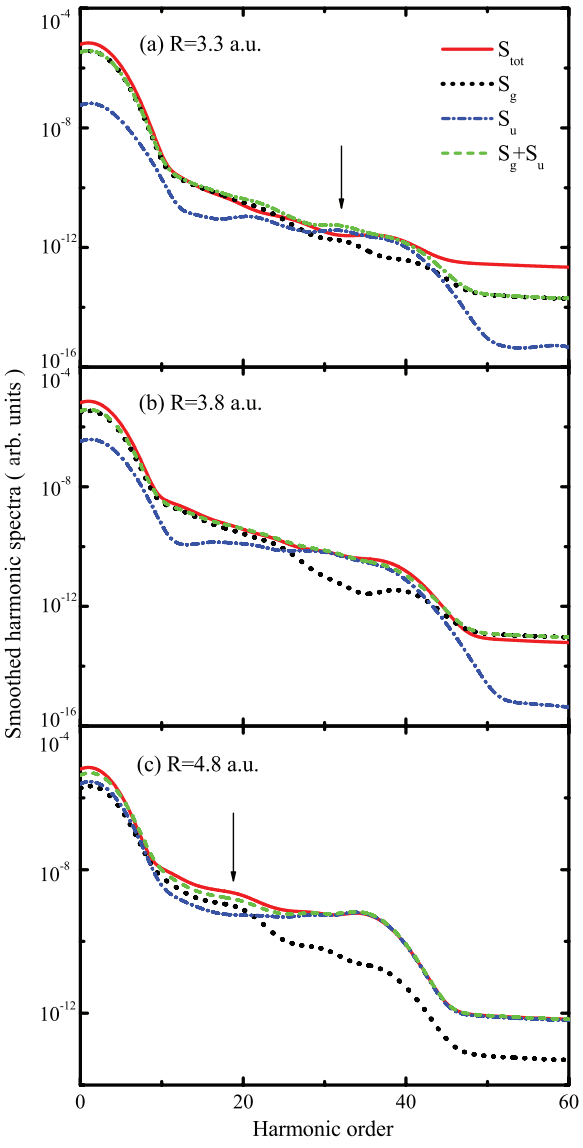

FIG. 4. (Color online) The smoothed spectrum components of the HHG spectra shown in Fig. 3. The arrows in panels (a) and (c) point to the location of the orbital interference minimum.

[38,39]. The ionization and the recombination to the σ_u state is enhanced as a result.

In Fig. 4 we show the smoothed spectrum components for the three cases of Fig. 3. The magnitude of $S_u(\omega)$ becomes greater and dominates in the plateau region with increasing R. This behavior is consistent with the above analysis. In addition, the effect of the orbital interference varies for different internuclear distances. At $R = 3.0$ a.u., the orbital interference suppresses the HHG spectrum around harmonic order 31, similar to the case at $R = 2.5$ a.u.; at $R = 3.8$ a.u., the effect of the orbital interference could be ignored; and at $R = 4.8$ a.u., the orbital interference induces some enhancement of the HHG spectrum around harmonic order 19.

IV. CONCLUSIONS

In this paper, we studied the role of the internuclear distance on the interference minimum in the HHG spectrum of H_2^+ based on full-dimensional TDSE calculations for the electronic degree of freedom. The contribution to the HHG spectrum was divided into three components corresponding to (i) recombination to the ground state, (ii) recombination to the first excited state, and (iii) the interference term between the amplitudes of the former two components. We compared the TDSE results and the two-center interference model and found that the two-center interference model works well when the internuclear distance is around the equilibrium where the coupling between the ground state and the first excited state is weak, such as in the cases for $R = 2.0$ and $R = 2.5$ a.u. When the internuclear distance is increased, recombination into the first excited state plays a more important role and the orbital interference term also needs to be taken into account and the two-center interference formula fails. The orbital interference could either suppress (e.g., at $R = 3.0$ a.u. and $R = 3.3$ a.u.) or enhance (e.g., at $R = 4.8$ a.u.) the HHG spectrum, and at some R (e.g., $R = 3.8$ a.u.) the orbital interference does not affect the shape of the spectrum. In general for larger internuclear distances and close to the cutoff in the harmonic spectra, the contribution associated with recombination to the σ_u state dominates.

We have found that the harmonic spectra of H_2^+ contains much information of the excited σ_u orbital, especially for larger internuclear distances with large dipole coupling between the ground and excited states. Extrapolating to many-electron systems, we expect an increased participation of excited states even in the nuclear equilibrium geometry for systems with high polarizability. In an adiabatic picture, this effect is equivalent to orbital distortion [40].

ACKNOWLEDGMENTS

L.B.M. acknowledges useful discussion with Maciej Dominik Śpiewanowski. This work was supported by the Fundamental Research Funds for the Central Universities [DUT12RC(3)60], the Danish Research Council (Grant No. 10-085430), and ERC-2011-StG (Project No. 277767).

[1] T. Brabec and F. Krausz, Rev. Mod. Phys. **72**, 545 (2000).
[2] C. Winterfeldt, C. Spielmann, and G. Gerber, Rev. Mod. Phys. **80**, 117 (2008).
[3] J. L. Krause, K. J. Schafer, and K. C. Kulander, Phys. Rev. Lett. **68**, 3535 (1992).
[4] P. B. Corkum, Phys. Rev. Lett. **71**, 1994 (1993).
[5] M. Lewenstein, P. Balcou, M. Y. Ivanov, A. L'Huillier, and P. B. Corkum, Phys. Rev. A **49**, 2117 (1994).
[6] P. Agostini and L. F. DiMauro, Rep. Prog. Phys. **67**, 813 (2004).
[7] G. Sansone, E. Benedetti, F. Calegari, C. Vozzi, L. Avaldi, R. Flammini, L. Poletto, P. Villoresi, C. Altucci, R. Velotta, S. Stagira, S. De Silvestri, and M. Nisoli, Science **314**, 443 (2006).

[8] J. J. Carrera, X. M. Tong, and S.-I. Chu, Phys. Rev. A **74**, 023404 (2006).
[9] E. Goulielmakis, V. S. Yakovlev, A. L. Cavalieri, M. Uiberacker, V. Pervak, A. Apolonski, R. Kienberger, U. Kleineberg, and F. Krausz, Science **317**, 769 (2007).
[10] F. Krausz and M. Ivanov, Rev. Mod. Phys. **81**, 163 (2009).
[11] J. Itatani, J. Levesque, D. Zeidler, H. Niikura, H. Pépin, J. C. Kieffer, P. B. Corkum, and D. M. Villeneuve, Nature (London) **432**, 867 (2004).
[12] C. B. Madsen and L. B. Madsen, Phys. Rev. A **76**, 043419 (2007).
[13] M. Lein, N. Hay, R. Velotta, J. P. Marangos, and P. L. Knight, Phys. Rev. Lett. **88**, 183903 (2002).
[14] M. Lein, N. Hay, R. Velotta, J. P. Marangos, and P. L. Knight, Phys. Rev. A **66**, 023805 (2002).
[15] M. Lein, Phys. Rev. Lett. **94**, 053004 (2005).
[16] G. L. Kamta and A. D. Bandrauk, Phys. Rev. A **71**, 053407 (2005),
[17] S. Baker, J. S. Robinson, M. Lein, C. C. Chiril, R. Torres, H. C. Bandulet, D. Comtois, J. C. Kieffer, D. M. Villeneuve, J. W. G. Tisch, and J. P. Marangos, Phys. Rev. Lett. **101**, 053901 (2008).
[18] O. Smirnova, Y. Mairesse, S. Patchkovskii, N. Dudovich, D. Villeneuve, P. Corkum, and M. Y. Ivanov, Nature (London) **460**, 972 (2009).
[19] X. Zhou, R. Lock, W. Li, N. Wagner, M. M. Murnane, and H. C. Kapteyn, Phys. Rev. Lett. **100**, 073902 (2008).
[20] B. K. McFarland, J. P. Farrell, P. H. Bucksbaum, and M. Gühr, Science **322**, 1232 (2008).
[21] W. Li, X. Zhou, R. Lock, S. Patchkovskii, A. Stolow, H. C. Kapteyn, and M. M. Murnane, Science **322**, 1207 (2008).
[22] S. Haessler, J. Caillat, W. Boutu, C. Giovanetti-Teixeira, T. Ruchon, T. Auguste, Z. Diveki, P. Breger, A. Maquet, B. Carré, R. Taïeb, and P. Salières, Nat. Phys. **6**, 200 (2010).
[23] C. Vozzi, M. Negro, F. Calegari, G. Sansone, M. Nisoli, S. D. Silvestri, and S. Stagira, Nat. Phys. **7**, 822 (2011).
[24] Y.-C. Han and L. B. Madsen, J. Phys. B **43**, 225601 (2010).
[25] S. Sukiasyan, C. McDonald, C. Destefani, M. Yu. Ivanov, and T. Brabec, Phys. Rev. Lett. **102**, 223002 (2009).
[26] S. Sukiasyan, S. Patchkovskii, O. Smirnova, T. Brabec, and M. Yu. Ivanov, Phys. Rev. A **82**, 043414 (2010).
[27] S. Odzak and D. B. Milosevic, J. Phys. B. **44**, 125602 (2011).
[28] B. B. Augstein and C. Figueira De Morisson Faria, Mod. Phys. Lett. B **26**, 1130002 (2012).
[29] J. Zhao and M. Lein, J. Phys. Chem. **116**, 2723 (2012).
[30] K. Burnett, V. C. Reed, J. Cooper, and P. L. Knight, Phys. Rev. A **45**, 3347 (1992).
[31] J. C. Baggesen and L. B. Madsen, J. Phys. B **44**, 115601 (2011).
[32] Y.-C. Han and L. B. Madsen, Phys. Rev. A **81**, 063430 (2010).
[33] T. K. Kjeldsen, L. A. A. Nikolopoulos, and L. B. Madsen, Phys. Rev. A **75**, 063427 (2007).
[34] T. K. Kjeldsen, Ph.D. thesis, Aarhus University, 2007, http://www.phys.au.dk/main/publications/PhD/Thomas_Kim_Kjeldsen.pdf.
[35] A. Etches, C. B. Madsen, and L. B. Madsen, Phys. Rev. A **81**, 013409 (2010).
[36] A.-T. Le, R. R. Lucchese, and C. D. Lin, Phys. Rev. A **82**, 023814 (2010).
[37] D. R. Bates, J. Chem. Phys. **19**, 1122 (1951).
[38] T. Zuo and A. D. Bandrauk, Phys. Rev. A **52**, R2511 (1995).
[39] G. Lagmago Kamta and A. D. Bandrauk, Phys. Rev. Lett. **94**, 203003 (2005).
[40] M. D. Śpiewanowski, E. Etches, and L. B. Madsen, (unpublished).